

ON THE INTERACTION BETWEEN THE MALVINAS CURRENT AND OCEAN MESOSCALE STRUCTURES AT 41°S

Camila Indira Artana¹, Martín Saraceno^{1,2,3}, Christine Provost⁴
camila.artana@cima.fcen.uba.ar

¹Departamento de Ciencias de la Atmósfera y los Océanos, FCEyN, UBA

²Centro de Investigación del Mar y la Atmósfera (CIMA/CONICET-UBA)

³Instituto Franco Argentino para el Estudio del Clima y sus Impactos (UMI-IFAECI/CNRS-CONICET-UBA)

⁴Laboratoire d'Océanographie et du Climat: Expérimentation et Approche Numérique (LOCEAN), UMR7159, Université Pierre et Marie

RESUMEN

La región donde ocurre la confluencia de las corrientes de Brasil y Malvinas es una de las regiones más energéticas del mundo. En esta zona se generan una gran cantidad de remolinos y meandros que migran hacia el sur y hacia el este y, solo en algunas ocasiones, hacia el sudoeste. En este último caso los remolinos son capaces de interactuar con la corriente de Malvinas. En este trabajo se investigó el rol que cumplen estas interacciones en la variabilidad del transporte de la corriente de Malvinas medido en 41°S (Spadone y Provost 2009). Haciendo uso de un criterio objetivo, se detectaron los máximos y mínimos de la serie de transporte. El análisis de los campos de la altura del mar satelital asociados a los eventos de mínimos y máximos indica que el 70% de los mínimos observados en el transporte de la corriente de Malvinas corresponden a actividad de mesoescala presente en las cercanías de la región en donde se midió el transporte. Por otro lado, el análisis del transporte de la corriente de Malvinas en otras latitudes, inferido a partir de datos de satélite únicamente, sugiere que los máximos están dominados por un forzante remoto. Este último resultado está limitado por la falta de datos in-situ al sur de 41°S.

ABSTRACT

The Brazil Malvinas-Confluence is one of the most energetic areas of the world. A great amount of eddies and meanders are generated in this area. Eddies migrate southward and eastward and, in some occasions, southwestward. In the last case they can approach the Malvinas Current and interact with its flow. In this work we investigated the role that mesoscale activity plays in controlling the variability of the time series of the transport of the Malvinas Current observed at 41°S (Spadone and Provost 2009). Extreme maxima and minima of the transport time series were detected with an objective criterion. Using satellite altimetry data we analyzed mean dynamic topography fields associated to each minimum and maximum detected. Results indicate that 70% of the minima in the transport time series are associated with the presence of mesoscale activity in the vicinity of the region where the Malvinas Current transport was measured. The analysis of the transport of the Malvinas Current using only satellite altimetry data at other latitudes suggests that a remote forcing process might be related to the largest maxima observed. In-situ measurements of the transport of the Malvinas Current at other latitudes are necessary to verify this result.

Key Words: Malvinas Current transport, ocean mesoscale, satellite altimetry.

1) INTRODUCTION

1.1 General circulation in the Southwestern Atlantic

The Southwestern Atlantic (SWA) ocean circulation is characterized by the encounter of the Malvinas Current (MC) with the Brazil Current (BC) (Figure 1). The MC is a branch of the Antarctic Circumpolar Current (ACC) (Piola and Gordon 1989). It flows northward along the Patagonian shelf break following approximately the 1000 m isobaths. It carries cold and relatively fresh waters (less than 7°C at surface in winter and approximately 34 PSU) up to 38°S where it encounters the BC. After the collision, the MC loops back into a cyclonic gyre to return southward to 55°W. The BC is the western boundary branch of the South Atlantic Subtropical gyre. It flows southward remaining in contact with the continental margin of South America and carrying warm and salty waters (higher than 26°C at the surface). The latitude at which it separates from the continental margin seems to have annual and semiannual variability, being further north during winters and further south during summers. Satellite IR images show that the latitude at which the BC separates from the 1000 m isobaths varies from 33°S to 38°S and the average latitude seems to be 36°S (Olson et al. 1988). After the BC separates from the coast it reaches the MC. The latitude at which they encounter also has seasonal changes (Matano et al. 1993) and large year-to-year variability (Goni and Wainer 2001). Using 9 years of AVHRR, Saraceno et al. (2004) showed that the confluence latitude is quite stable (near 39.5°S 53.5°W). However, the orientation of the merged front changes from season to season, from N-S in winter to NW-SE in summer. After they met, the BC separates in two branches: one of them flows northward describing a recirculation cell, and the other one conforms the overshoot, flowing southwards and then turning to the northeast at 45°S (Peterson and Stramma 1991). The area of convergence of these two currents is known as Brazil-Malvinas Confluence (BMC) (Gordon and Greengrove 1986). This region is one of the most energetic zones of the world ocean: Eddy Kinetic Energy (EKE) is higher than 1700 cm²s⁻². A great amount of eddies are generated at the Confluence (Garzoli and Garrafo 1989). These eddies are able to transport different characteristics such as mass, temperature, salinity, phytoplankton and other properties from the region of generation to other very far regions (e.g. Chelton et al., 2007, 2011). The observed distribution of eddies is in agreement with the generation of eddies from meanders of the above-mentioned currents: cyclonic (anticyclonic) eddies might detach from a meander of the current on the left (right) side when looking downstream on the current (Saraceno and Provost, 2012). From the confluence region most eddies migrate southward and eastward, only few move southwestward (Saraceno and Provost, 2012). As a consequence the MC area has relatively low EKE values. The few eddies that do move southwestward might interact with the MC. Spadone and Provost (2009) have shown that these eddies are responsible of the largest fluctuations on the MC transport measured at 41°S. In this work we explored with more detail all the fluctuations of the MC transport at this latitude. We observed that in many cases a significant decrease in the transport time series is related with the presence of mesoscale activity close to the position where the MC transport was measured. One of the main reasons that motivate the study of the MC and its fluctuations is that the MC is a major source of nutrients that sustain large fisheries in the SWA. Moreover, the MC is part of the Meridional Overturning Circulation (MOC) and it contributes to regulate the climate since it helps the exchange of heat and salt through water mass transformation in the Argentine Basin (Lumpkin 2007). Therefore, understanding the origin of MC transport fluctuations is an important task.

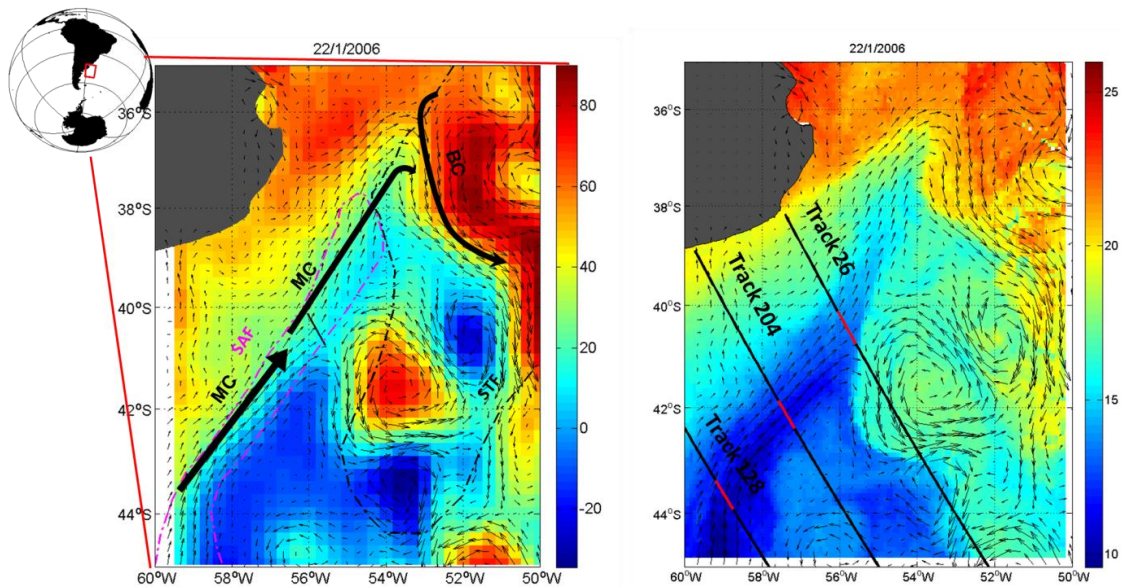


Figure 1: Left panel: Mean Absolute Dynamic Topography (MADT) for the week centered on the 22nd of January 2006. The mean positions of the Subtropical Front (STF) and the Subantarctic Front (SAF) are from Saraceno et al. (2004) and are indicated by black and magenta dash-dotted lines. The general circulation of the region is shown with black arrows. Right panel: Sea Surface Temperature (SST) (°C) for the same date of the left panel. Black lines show Jason-2 altimeter tracks; the red portion of the lines along the satellite tracks represent the section across which we calculated the MC transport.

2) DATA AND METHODS

2.1 Satellite altimetry data

We used two types of altimetry data produced by Ssalto/Duacs and distributed by AVISO (<http://www.aviso.oceanobs.com>): Maps of sea surface height (SSH) and of absolute mean dynamic topography (MADT) for the region comprised between 60-35°W, 45-35°S and for the period for which the MC transport was inferred by Spadone and Provost (2009): 1992 to 2008. These gridded maps have a 7-day temporal sampling and a spatial resolution of 1/3° x 1/3° which allows to detect eddies with radii larger than 40km (Chelton et al., 2011). Geostrophic velocities were derived from the MADT and SSH fields.

2.2 Sea surface temperature

We used sea surface temperature (SST) data from the Moderate Resolution Imaging Spectro Radiometer (MODIS) ocean-color sensor on board of the Aqua satellite, which measures visible and infrared radiation in 36 wavebands. We employed level 3 data downloaded from <http://oceancolor.gsfc.nasa.gov/>. The images that we used have a spatial resolution of 9 km and a temporal resolution of 8 days. These fields allowed a greater level of detail in the study of the special events detected; although in some cases cloud coverage prevented the observation of the area of interest.

2.3 Malvinas current transport

To identify the largest fluctuations of the MC we used a 14-year-long (1992-2008) time-series of the transport of the MC (Figure 2) provided by Spadone and Provost (2009). The time series was estimated based on the good correlation obtained between transport estimation from current meters deployed at 41°S and from satellite altimetry. The instruments were located at 40°- 41°S, below Jason-1 track 26, during two different periods: December 1993 to June 1995 and December 2001 to February 2003. In both periods the correlation between transport time series computed using current meters only and combining altimetric and in-situ data is high (0.7). Spadone and Provost (2009) showed that the transport time series suffered a strong shift: from 1992 until 1997 variability was more concentrated in periods that oscillate between 50 and 90 days while after 2000 long periods such as the seasonal one dominate.

In order to detect extreme events in the MC transport we defined an objective criterion that can be summarized as follows: first we applied a two years low pass filter on the transport series; then an extreme event was defined considering those minima and maxima that overpassed three times the standard deviation of the low-pass filtered time series. Figure 2 shows the time series of MC transport with the 45 minima and 50 maxima that were detected following the above described procedure.

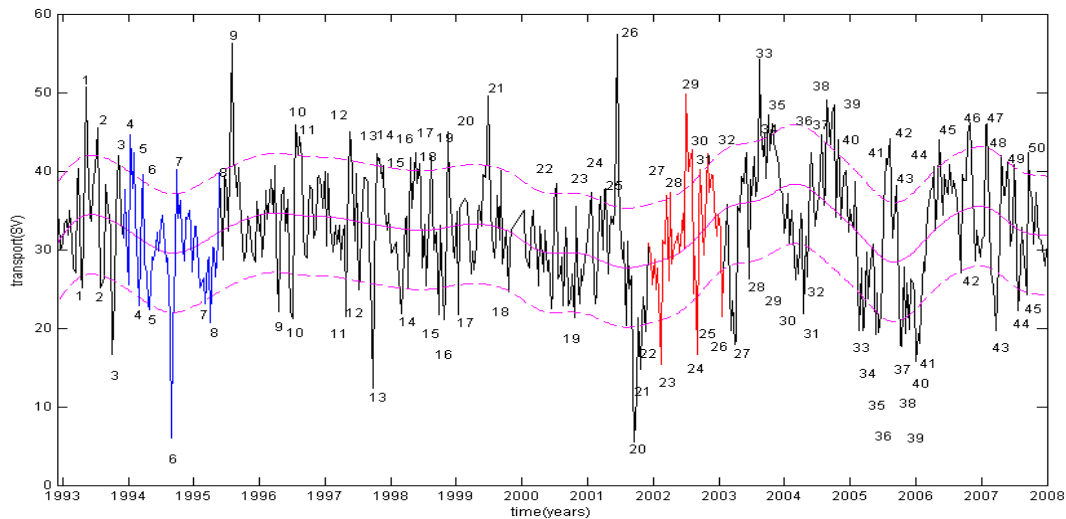


Figure 2. Black line shows the time series of the transport of the MC. Magenta solid line shows a 2 years low pass filter and magenta dash-dotted lines show the mean plus (minus) three times the standard deviation. Blue and red lines indicate the period of the mooring (1993-1995 and 2001-2003 respectively).

3) RESULTS

The spatial distribution of eddies in the region has been analyzed by Saraceno and Provost (2012). Their figure 3 clearly shows that there are no eddies close or nearby the MC. Chelton et al. (2011) also found a similar result in a global-scale analysis. It is possible that this absence of eddies is due to the method used by the authors to detect eddies. A close inspection of altimetry images shows that in some regions along the eastern side of the MC it is possible to visualize mesoscale structures that look like eddies. The hypothesis to be tested in this article is that those mesoscale structures are responsible for a large portion of the MC transport variability.

To investigate if there is mesoscale activity close to the MC at 41°S we analyzed the spatial distribution of the frequency of occurrence of events in which the horizontal gradient of SSH presented large values (Figure 3). This frequency was calculated as follows:

- i) For all minima and maxima identified in the transport time series (Figure 2), we computed the field of horizontal gradient of SSH;
- ii) For each field of (i) we calculated the histograms of horizontal gradient of SS;
- iii) We fitted each of the histograms computed in (ii) with a Gaussian curve;
- iv) For each fitted curve of (iii) we found the value corresponding to the positive inflection point of the Gaussian curve;
- v) We used the values calculated in (iv) as a threshold for the absolute value of SSH gradients;
- vi) We built binary maps: Unitary values were assigned to pixels which absolute value of SSH gradient was larger than the threshold defined in (iv). The rest of the pixels were set to zero.
- vii) Two sets of binary maps were created: one composed by the binary maps corresponding to the dates with a minimum of the transport and the other composed by the binary maps corresponding to the dates with a maximum of the transport.
- viii) We calculated, for each set of (vii), the sum of the binary maps.
- ix) We normalized maps computed in (viii) and multiplied values per 100.

Following the above described procedure we obtained the two maps displayed on Figure 3. The right panel of Figure 3 (corresponding to the composite of minima) shows that there is a region with values larger than 70%, ie where the edge of a mesoscale feature has been detected in at least 70% of the cases in which the MC had a minima, following the methodology described above. The aforementioned region is in the proximity of the moorings, but do not overlap the mooring section where the MC has been measured. However, the geostrophic velocities fields associated to these mesoscale events can interact with the MC flow at 41°S. This is clearly illustrated in Figure 1: SSH gradients associated to the mesoscale structure located at 42°S and 54°W are well separated from the mooring line. However, the geostrophic currents associated to this mesoscale structure clearly indicate that the MC flow across the mooring line is affected by the vicinity of the mesoscale feature at 42°S and 54°W.

The left panel of Figure 3 corresponds to the composite of the maxima of transport detected in Figure 2. The values observed are in general lower than those of computed with the minima (right panel of Figure 3), and they are located farther north from the mooring section. The number of events is quite low in the region where the interaction could take place (neighborhood of the mooring line), suggesting that very few cases corresponding to maxima in the transport time series are associated with mesoscale activity there.

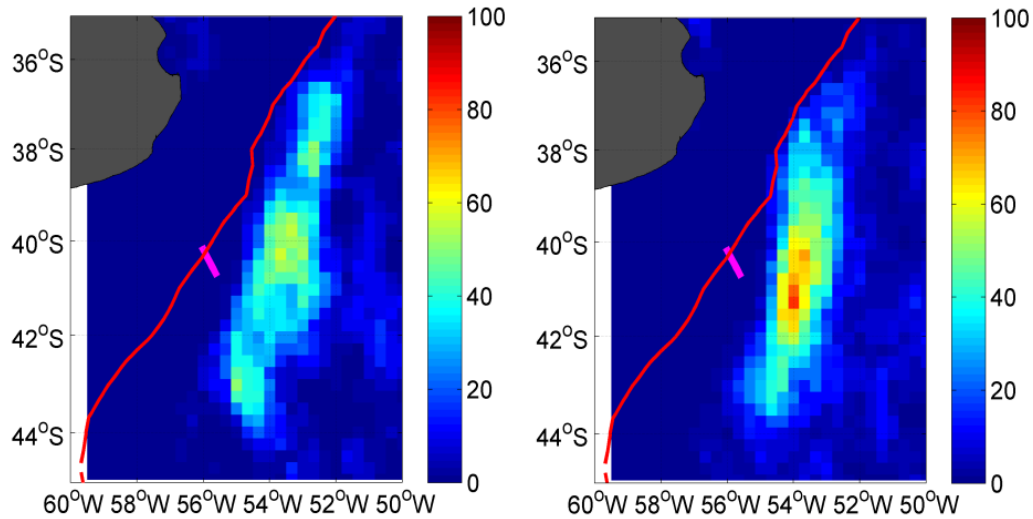


Figure 3: Frequency of occurrence of events in which the horizontal gradient of SSH presented high values for the dates of maxima (left) and minima (right). The red line represents the 1000 m isobath and the magenta line the section across which the transport was measured.

To further explore the spatial distribution of the MADT and sea surface geostrophic velocity associated to these events we constructed averages of these variables for the dates of minima and maxima (Figure 4). Minima are characterized by the presence of an anticyclonic eddy near the section across which the transport of the MC was measured. On the other hand, there are no eddies close to the MC for the average corresponding to the maxima.

The two fields also suggest that the northern portion of the STF (identified with a blue line in the averages of Figure 4) has a very different orientation in each case. In the minima average, it has a NW-SE orientation, while for the maxima average the orientation is meridional. Therefore, maxima events are characterized by the absence of eddies and by a meridional position of the STF front; while minima events are characterized by the presence of eddies in the vicinity of the MC and by a more zonal position of the STF. As the STF in this region change his orientation from N-S in winter to NW-SE in summer (Saraceno et al, 2004), we investigated if the occurrence of minima and maxima also has a seasonal behavior. However, the monthly climatology of SSH for the dates corresponding to minima and maxima in the MC transport does not indicate the presence of a seasonal pattern (not shown).

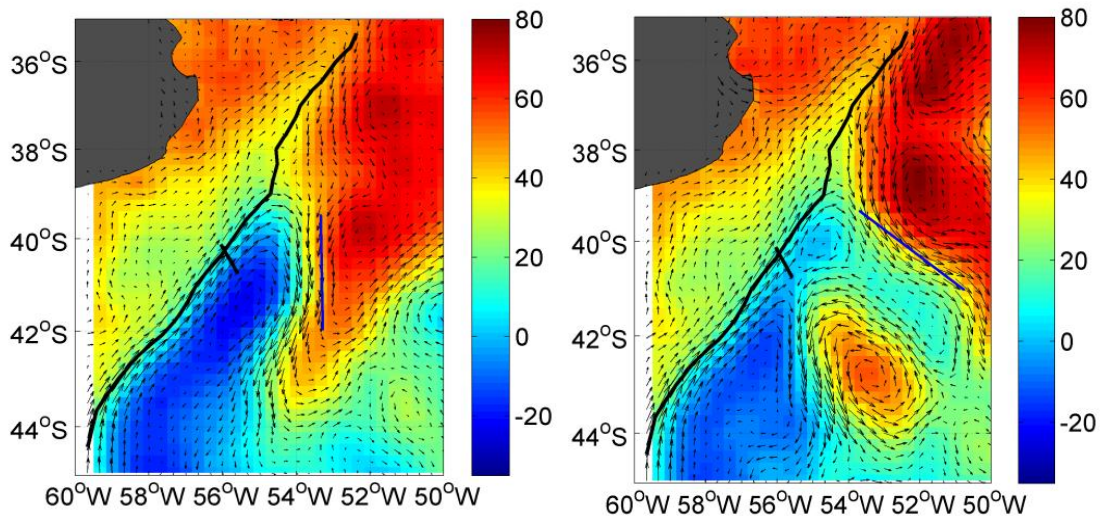


Figure 4. Average of MADT and geostrophic velocities for the dates corresponding to minima (right panel) and maxima (left panel) of the MC transport. The arrows show the geostrophic velocities. The STF and the section across which the transport was measured are represented by a blue and a black line respectively.

As the maxima do not seem to be related with mesoscale activity, we proposed another hypothesis for these events. We investigated the possibility that the increase registered across track 26 was due to an increase in the whole flow. To test this hypothesis we calculated the transport time series across tracks 204 and 128, located southward from track 26 (Figure 1, left panel): assuming that MC has a barotropic vertical structure we calculated the transport in the upper 1500 m using surface geostrophic velocities derived from altimetry data only. We then applied a 60-day low-pass filter to the three transport time series in order to eliminate mesoscale effects. Figure 5 shows the transport across the three tracks. As we can see, in most cases an increase in transport across track 26 is accompanied with an increase across tracks 128 and 204. What makes the time series of track 26 different from those obtained on tracks 128 and 204 are the largest minima, which are present in track 26 but not in the other two. These minima (represented with asterisks in Figure 5) are associated with the presence of eddies that are very long lasting, therefore allowing them to survive to the 60 day filter. To confirm these observations we calculated the correlation between the transports time series between all the tracks (Table II). Correlations are higher between transports across tracks 128 and 204 and lower between track 26 and track 128 and 204. The correlations between transport time series across tracks 128 and 204 increase considerably if we computed without considering the minima indicated with an asterisk in Figure 5 (Table II). This confirms the idea that a local mechanism affects the variability of MC transport along track 26 and that the origin of the maxima observed in the three sections is not related to mesoscale features. Vivier and Provost (2001) suggested that the MC transport has local and remote forcing: the local forcing is the result of changes in the wind stress curl around 40°S and the remote forcing is related with negative wind stress curl anomalies at Drake Passage with a lag of 20-30 days.

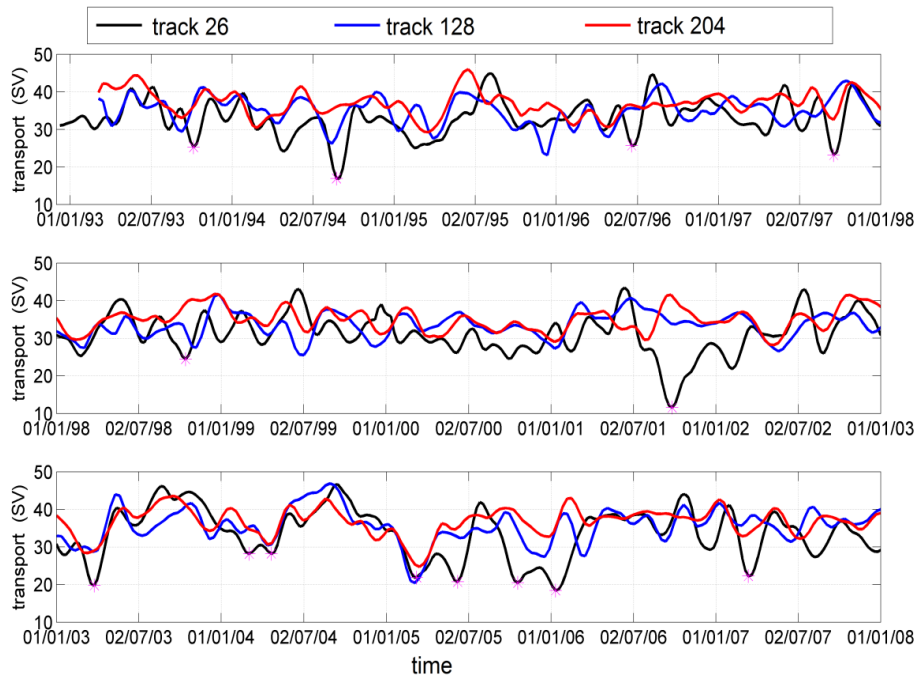


Figure 5. Transport along tracks 26 (black), 128 (blue) and 204 (red), smoothed with a 60 day low-pass filter. Minima from transport along track 26 associated to mesoscale activity are represented with magenta asterisks.

	Between the original low-pass time series	Suppressing values in Track 26 corresponding to transport minima
Track 26-Track128	0.29	0.39
Track 26-Track 204	0.27	0.41
Track 128-Track 204	0.62	0.62

Table II. Correlation between transport along track 26, 128 and 204 for the original series (column 2) and for the case where the minima of track 26 were replaced by NaN (column 3). In all cases the correlation was significant (95% of confidence level).

4) SUMMARY AND DISCUSSION

Extreme maxima and minima of the time series of MC transport were detected using an objective criterion. We identified 45 minima and 50 maxima. We observed that 70% of the events of minima were related with the presence of mesoscale features generated at the BMC that occasionally migrate southwestward and could obstruct the MC flow at 41°S, where the transport time series was obtained. However, even if we observed a coincidence between mesoscale activity and transport minima, the causality relation is not yet established and further studies are needed to prove this idea. In this sense, the following question is still open: is the decrease in MC transport due to the presence of mesoscale activity interacting with the current, or is the weakening of the transport allowing eddies (mesoscale) to settle near the current? Matano et al. (1993) and Agra and Nof (1993) showed with numerical simulation experiments that a decrease in MC transport is accompanied by a southward migration of the latitude of the BMC. This result is in agreement with the fact that minima events are those related with the presence of mesoscale activity close to the MC, since in these cases the confluence migrates southward and eddies generated at this region are closer to the region where the transport was measured.

Vivier and Provost (2001) investigated the possible sources of the variability of the transport of the MC. The processes considered in their analysis included: the strength of the ACC, wind forcing on a regional scale (south of the Drake Passage), wind forcing on a circumpolar scale, and fluctuations of the BC. They distinguished two sources of variability: a local mode and a remote mode. The local mode is related with changes in the wind stress curl around 40°S. However, this contribution to the variability is low. Mesoscale activity was not considered as a local forcing of the variability of the MC transport in their analysis. In our work, we observed that these features should be considered as a local source of variability of the transport of the MC, as 70% of the events of minima were related with the presence of mesoscale activity.

On the other hand, Vivier and Provost (2001) showed that the remote mode is related with an increase in transport associated to negative wind stress curl anomalies at Drake Passage with a lag of 20-30 days. This is in agreement with our observation that suggests that the largest maxima of the transport of the MC are not related to local mesoscale process but to remote forcing process.

Finally, we wish to highlight that the southern estimations of the transport across the MC were made without considering in-situ data. A validation of the altimetry data with in-situ measurement is necessary to corroborate/refute the transport time series in the southern sections.

ACKNOWLEDGMENTS:

Altimeter data and the mean dynamic topography were provided by AVISO (<http://www.aviso.altimetry.fr>). This work is part of the following projects: ECOS- Sud A14U02, EUMETSAT/CNES DSP/ OT/12–2118 and CONICET-YPF PIO 133–20130100242. CA participation to CONGREMET was supported by CONICET-YPF PIO 133–20130100242.

5) REFERENCES

- Agra, C. & Nof, D., 1993:** Collision and separation of boundary currents. *Deep Sea Research Part I: Oceanographic Research Papers*, 40(11), 2259-2282.
- Chelton, D. B., Schlax, M. G., Samelson, R. M., & de Szoeke, R. A., 2007:** Global observations of large oceanic eddies. *Geophysical Research Letters*, 34(15).
- Chelton, D. B., Schlax, M. G., & Samelson, R. M., 2011:** Global observations of nonlinear mesoscale eddies. *Progress in Oceanography*, 91(2), 167-216.
- Franco, B. C., Piola, A. R., Rivas, A. L., Baldoni, A., & Pisoni, J. P., 2008:** Multiple thermal fronts near the Patagonian shelf break. *Geophysical Research Letters*, 35(2).
- Garzoli SL & Garrafo Z., 1989:** Transports, frontal motions and eddies at the Brazil-Malvinas Currents Confluence. *Deep Sea Res* 36:681-703
- Goni, G. J., & Wainer, I., 2001:** Investigation of the Brazil Current front variability from altimeter data. *Journal of Geophysical Research: Oceans* (1978–2012), 106(C12), 31117-31128.
- Gordon, A. L., 1989:** Brazil-Malvinas Confluence–1984. *Deep Sea Research Part A. Oceanographic Research Papers*, 36(3), 359-384.
- Gordon, A. L., & Greengrove, C. L., 1986:** Geostrophic circulation of the Brazil-Falkland confluence. *Deep Sea Research Part A. Oceanographic Research Papers*, 33(5), 573-585.
- Ladd, C., Stabeno, P., & Cokelet, E. D., 2005:** A note on cross-shelf exchange in the northern Gulf of Alaska. *Deep Sea Research Part II: Topical Studies in Oceanography*, 52(5), 667-679.
- Lumpkin, R., & Speer, K., 2007:** Global ocean meridional overturning. *Journal of Physical Oceanography*, 37(10), 2550-2562.
- Matano, R. P., 1993:** On the separation of the Brazil Current from the coast. *Journal of physical oceanography*, 23(1), 79-90.
- Matano, R. P., Schlax, M. G., & Chelton, D. B., 1993:** Seasonal variability in the southwestern Atlantic. *Journal of Geophysical Research: Oceans* (1978–2012), 98(C10), 18027-18035.
- Matano, R. P., & Palma, E. D., 2008:** On the upwelling of downwelling currents. *Journal of Physical Oceanography*, 38(11), 2482-2500.
- Matano, R. P., Palma, E. D., & Piola, A. R., 2010:** The influence of the Brazil and Malvinas Currents on the southwestern Atlantic shelf circulation. *Ocean Science*, 6(4), 983-995.

Moore, T. S., Matear, R. J., Marra, J., & Clementson, L., 2007: Phytoplankton variability off the Western Australian Coast: Mesoscale eddies and their role in cross-shelf exchange. *Deep Sea Research Part II: Topical Studies in Oceanography*, 54(8), 943-960.

Olson, D. B., Podestá, G. P., Evans, R. H., & Brown, O. B., 1988: Temporal variations in the separation of Brazil and Malvinas Currents. *Deep Sea Research Part A. Oceanographic Research Papers*, 35(12), 1971-1990.

Piola, A. R., & Gordon, A. L., 1989: Intermediate waters in the southwest South Atlantic. *Deep Sea Research Part A. Oceanographic Research Papers*, 36(1), 1-16.

Piola, A. R., Avellaneda, N. M., Guerrero, R. A., Jardón, F. P., Palma, E. D., & Romero, S. I., 2010.: Malvinas-slope water intrusions on the northern Patagonia continental shelf. *Ocean Science*, 6(1), 345.

Piola, A. R., Franco, B. C., Palma, E. D., & Saraceno, M., 2013: Multiple jets in the Malvinas Current. *Journal of Geophysical Research: Oceans*, 118(4), 2107-2117.

Peterson, R. G., & Stramma, L., 1991: Upper-level circulation in the South Atlantic Ocean. *Progress in Oceanography*, 26(1), 1-73.

Saraceno, M., Provost, C., Piola, A. R., Bava, J., & Gagliardini, A., 2004: Brazil Malvinas Frontal System as seen from 9 years of advanced very high resolution radiometer data. *Journal of Geophysical Research: Oceans (1978–2012)*, 109(C5).

Saraceno, M., & Provost, C., 2012: On eddy polarity distribution in the southwestern Atlantic. *Deep Sea Research Part I: Oceanographic Research Papers*, 69, 62-69.

Spadone, A., & Provost, C., 2009: Variations in the Malvinas Current volume transport since October 1992. *Journal of Geophysical Research: Oceans (1978–2012)*, 114(C2).

Vivier, F., & C. Provost, 1999: Direct velocity measurements in the Malvinas Current. *J. Geophys. Res.*, 104, 21,083– 21,103, doi:10.1029/ 1999JC900163.

Vivier, F., Provost, C., & M. P. Meredith, 2001: Remote and local forcing in the Brazil-Malvinas region. *Journal of physical oceanography*, 31(4), 892-913.